A Geochemical Study of Acid Mine Water from a Pyrite Mine, North Wales.

By J.M. Pearce and S.J. Kemp.

Mineralogy and Petrology Group, British Geological Survey,
Kingsley Dunham Centre, Keyworth, Nottingham, NG12 5GG, United Kingdom.

ABSTRACT

This paper presents the results of a geochemical study of acid mine waters and related precipitates, sampled at the Cae Coch disused pyrite (FeS_2) mine in Gwynedd, North Wales. The programme aimed to investigate the concentration of selected trace elements, including rare-earth elements, uranium and thorium in solution, and their interaction with iron-bearing minerals. All mine waters analysed are iron-rich and are associated with a variety of precipitates including goethite (α-FeOOH) and X-ray amorphous iron oxyhydroxides.

The groundwater samples can be divided into two groups; those of approximately neutral pH that represent rapid infiltration of meteoric water into the mine and those of low pH which have developed as a result of pyrite oxidation. Extensive goethite deposits, precipitated from the acid mine drainage, contain high concentrations of many trace elements. Drips through the mine roof, however, have precipitated stalactites of amorphous iron oxyhydroxide which have higher concentrations of barium, lead, nickel and uranium. Gypsum forms extensive efflorescence on drier surfaces and was found to be preferentially enriched in light rare-earth elements, in contrast to the amorphous iron oxyhydroxide which is preferentially enriched in heavy rare-earths. The relative ability of the goethite and X-ray amorphous iron oxyhydroxide precipitates in removing toxic trace elements from solution within an acid mine drainage environment is discussed.

INTRODUCTION

The sorption of trace elements onto Fe-rich phases commonly formed in acid mine drainage (AMD) has been extensively studied in recent years in connection with heavy metal contamination [e.g. 1 and 2] and in laboratory simulations [e.g. 3 and 4]. However, little information is available on the relative importance of different Fe-rich phases in removing trace elements from very acidic (pH <3.5) groundwaters. In particular, little is known about the behaviour of the rare-earth elements (REE) in these systems. Most previous studies have investigated such sorption processes in AMD systems at near-neutral pH, due to dilution of the AMD by unpolluted surface waters.

Pearce & Kemp - A Geochemical Study of Acid Mine Drainage from a Pyrite Mine, North Wales.

As part of their wide ranging investigations into a radioactive waste repository UK Nirex Ltd. are conducting a number of studies into the geochemistry of disturbed natural systems. This paper presents data on the geochemistry and mineralogy of AMD precipitates from a disused pyrite (FeS_2) mine in North Wales. Changes in the trace element composition and mineralogy along the AMD flowpath are also investigated.

DESCRIPTION OF SITE

The Cae Coch massive pyrite mine, Gwynedd, North Wales (SH 775 653), penetrates a folded stratiform mass of quartzose pyrite ore lying at the junction of the Ordovician Dolgarrog Volcanic Formation and the overlying Llanrychwyn Slates. The Dolgarrog Volcanic Formation comprises basaltic hyaloclastites, basalts and basaltic crystal tuffs. The Llanrychwyn Slates are cleaved pyritic mudstones. Mining occurred on a small scale between 1860-75 and 1916-18 [5]. One arm of the folded orebody has been worked out forming a steeply sloping cavern.

The drainage system within the mine is dominated by two streams. The larger of these drains the top of the mine, where numerous rapid drips coalesce. An exploratory adit extends from the main cavern for approximately 200 metres and is drained by a second, smaller stream which joins the main flow in the cavern. A large adit at the lowest part of the mine provides an outlet for the AMD. The rest of the cavern is relatively dry except for isolated minor drips and stagnant pools. Where water flow is reduced, flowstones of fine, buff-brown, clay-like material are well developed. A thick (30-40 cm) accumulation of orange, soft, laminated goethite (α-FeOOH) has developed where the stream flows along a horizontal bed. Drips through the mine roof have formed iron oxyhydroxide straws, up to 20 cm in length.

Encrustations of pale blue, translucent melanterite ($FeSO_4.7H_2O$) cover many of the exposed mudstone surfaces and may develop into thick and extensive coatings as a result of continued evaporation from the humid atmosphere. The exposed pyrite-rich shale and pyrite orebody generally appeared to be fresh or slightly tarnished by sub-aerial oxidation. In places, gypsum ($CaSO_4.2H_2O$) efflorescences are associated with surface alteration of the pyrite ore in the moist atmosphere.

METHODOLOGY

The mine was visited in January and June 1991. Waters, precipitates and alteration products, associated with the AMD system, were sampled from a variety of locations within the mine. Water samples were collected from roof drips, from flowing AMD streams and from stagnant pools. To minimise contamination, the water was sampled prior to any solid sampling. Eh and pH of the waters were determined by specific electrodes using a sealed perspex flow-through cell, through which water was drawn by syringe. The conductivity of the waters was measured on site. Bicarbonate concentration was determined by titration with sulphuric acid. Groundwater samples were filtered through a 0.45 μm nylon Acrodisk filter and preserved for subsequent laboratory analysis of major, minor and trace elements. Groundwater compositions are presented in Table 1.

Near monomineralic phases were hand-separated from precipitates and alteration products, and their mineralogy confirmed by X-ray diffraction (XRD). Polished thin sections were also prepared and examined by backscattered scanning electron microscopy (BSEM). Chemical analyses of the precipitates are presented in Table 2.

Major and trace cation concentrations in both water and solid samples were analysed using an inductively coupled plasma-optical emission spectrometer (ICP-OES). Pb, Cd and Mo were determined by atomic absorption spectroscopy (AAS) REE, U and Th were determined using an inductively coupled plasma mass spectrometer (ICP-MS). Total organic carbon and total inorganic carbon were measured by Shimozu TOC analyser. U and Th analyses were carried out at ICI, Billingham by induced neutron activation analysis (INAA).

Samples for XRD analysis were ground with a pestle and mortar to pass a 125 μm sieve. Where possible, to preserve the hydration state of the materials, the samples were run 'as sampled'. XRD analyses were carried out using an automatic diffractometer using Co-Kα radiation, operating at 45 kV and 40 mA and scanning over the range 3-50 °2θ at a scan speed of 0.9° 2θ/minute.

BSEM examination was carried out using a scanning electron microscope fitted with a four element solid-state (diode) backscattered electron detector. A qualitative energy-dispersive X-ray microanalyser (EDXA), fitted to the SEM, was used to aid mineral identification.

Saturation indices (SI) were calculated using the EQ3NR geochemical code and EQ3NR database [6]. HCO_3^- was not detected in any of the AMD samples and hence log fCO_2 was set to an atmospheric value. In all other samples the reported HCO_3^- levels were used. In addition to SI

calculations, EQ3NR was used to determine the Fe concentration at which saturation of specific phases occurred. The value of log fO_2 was set at two different values in some groundwaters to determine its effect on speciation. These were equilibrated with atmospheric O_2 and a value based on the Fe^{2+}/Fe^{3+} redox couple, as derived by the code. Measured Eh values were not used since they were not thought to be representative. Changes in log fO_2 had very little influence on element speciation nor did it affect the relative proportions of these species. This is expected since Fe^{2+} would not be important in groundwaters in contact with the atmosphere.

RESULTS

The waters may be split into two broad groups based on their chemistries and spatial distribution in the mine (Table 1). The first group ("inflow waters") were collected from roof drips and essentially represent meteoric waters that have drained through fissures and joints. One sample (CC6) has reacted to a limited extent with the oxidising pyrite. These Ca-Na-HCO_3-Cl dominated, inflowing waters have pH values in the range 6.0 to 8.0 and Eh is between 302 to 868 mV. These dilute groundwaters typically have much lower major and trace element concentrations (particularly with respect to Ca, Mg, SO_4^{2-}, Si, Fe, Mn, Al, Ni, Cu, Zn, Cr, V, As, REE, Th and Y) than the outflowing AMD. Cd, Co, Cr, Cu, Pb, Ni, V and Zn were below detection in these inflowing groundwaters. Ba concentrations are in the range 0.05 to 0.12 ppm and Sr in the range 0.06 to 0.27 ppm. Total REE levels vary from 0 to 0.18 ppb. U concentrations are in the range 1 to 13.6 ppb.

The second group of waters have pH values within the range 2.1 to 2.7 and Eh values between 491 to 883 mV. These waters are essentially Fe-SO_4^{2-} dominated and represent interaction with the oxidising pyrite ore to produce AMD. Total Fe and SO_4^{2-} concentrations are increased by up to three and four orders of magnitude respectively, relative to the inflowing waters. The concentrations of some major cation species increase dramatically in the AMD (Table 1) providing evidence for enhanced leaching of the shales and pyrite ore, in particular of feldspars and clay minerals. For example, SiO_2 is increased two- to three-fold relative to the inflowing drips. Al increases from below detection in the inflowing waters to 26 to 89 ppm in AMD. Ca and Mg similarly increase three- to fourfold and four- to six-fold, respectively. REE and Th concentrations were high relative to the inflowing waters but U values were comparable to those of the inflow waters. Many heavy metals remained below detection limits or at low concentrations in the AMD - for example Cd, Co, Cr, Ni, Pb, V and Zn. This is not surprising for Cd and Pb since concentrations were < 1ppm and <10 ppm in samples of weathered shale from within the mine. However, Co, Cr, Ni, V and Zn concentrations were relatively high in samples of weathered shale. This suggests that if dissolution of these heavy metals is taking place they are then being rapidly removed from solution by the Fe-

rich precipitates. This is confirmed by analyses of the goethite and amorphous Fe oxyhydroxides samples. Nevertheless the AMD contained slightly higher Cr, Ni, V and Zn concentrations than the inflowing waters. Ba and Sr concentrations did not increase in concentration in the AMD. Sr is likely to be coprecipitated with gypsum and the low solubility of $BaSO_4$ will result in rapid Ba reprecipitation as barite.

Samples CC2 and CC12 were taken from the same AMD pool but on separate visits to the mine (January and June respectively). On the first visit water levels and flow rates were generally much lower than during the second visit when there was evidence of widespread flooding of the mine cavern to a depth of approximately 10 centimetres. The chemistries of the two samples reflect the changes in drainage. Under low-flow conditions the pool had a very low pH (2.7) and high trace element concentrations. However with increased flow due to prolonged rainfall, the AMD was diluted in this area (pH 7.8). This has wider implications for the drainage in the rest of the mine which is also likely to be flushed in periods of heavy rainfall. This suggests that groundwater chemistries of the AMD are likely to be strongly influenced by fluctuations in flow-rate due to changes in weather conditions.

Two goethite samples were collected. XRD analysis indicated that these were essentially pure, containing only trace quantities of quartz. Quartz does not contain significant trace elements and is considered to have little influence on the goethite composition data (Table 2). The goethites contain 28 and 29 ppm Co, 37 and 35 ppm Cr, 63 and 29 ppm Cu, 16 and 0 ppm Ni, 84 and 172 ppm V, 73 and 37 ppm Zn, <10 ppm Pb, 29 and 8 ppm Ba, and 5 and 2 pm Sr. Total REE concentrations were 19.63 and 3.83 ppm with U and Th below detection (< 1ppm) in both samples.

In addition to goethites, samples of Fe-rich stalactites were also collected. Their X-ray amorphous nature suggests they are composed of a poorly-crystalline Fe oxyhydroxide. The most common of these is ferrihydrite (approximately $Fe_2O_3.2FeOOH.2.6H_2O$) [7, 8, 9]. However, we have no conclusive evidence that the amorphous precipitates analysed in this study were ferrihydrite as described in the studies listed above. Chemical analysis (Table 2) indicates that the sample contains significant Ba (2428 ppm) and Sr (190 ppm). In addition, some transition elements are enriched in this material - e.g. Ni (226ppm), Zn (87 ppm) and Pb (235 ppm). Co concentrations are comparable with the goethite samples at 29 ppm. Y concentration is relatively high in the amorphous Fe oxyhydroxide, 133.4 ppm compared to 4.1 and 0.5 ppm in the goethite samples. U concentration is 3 ppm and Th was not detected. Total REEs are 43.83 ppm.

Pearce & Kemp - A Geochemical Study of Acid Mine Drainage from a Pyrite Mine, North Wales.

The melanterite efflorescence was shown by XRD analysis to contain trace amounts of gypsum. Compared to other precipitates, melanterite is relatively enriched in Cu (115 ppm). Co (c. 25 ppm) concentrations are similar to both those in the goethite and amorphous Fe oxyhydroxide samples. Cr (13 ppm), Pb (16 ppm), V (23 ppm) and Zn (32 ppm) concentrations are lower than in the goethite and amorphous Fe oxyhydroxide samples. Ni concentrations (30 ppm) are intermediate between goethite and amorphous Fe oxyhydroxide. Ba and Sr concentrations are relatively low (25 and 1 ppm). Total REEs (ca. 1 ppm) are very low and U and Th are below detection limits (< 1 ppm). Melanterite, although an important alteration product of AMD, is highly soluble and will therefore readily dissolve on contact with the groundwater.

The gypsum samples also contain trace quartz. Chemical analysis (Table 2) indicates significant Fe is present possibly as natrojarosite ($NaFe_3[SO_4]_2[OH]_6$) and amorphous Fe oxyhydroxide contaminants. Trace metals are present in similar concentrations to those in the melanterite (Table 2). Co concentrations are slightly lower than in the goethite and amorphous Fe oxyhydroxide samples. U and Th are below detection limits (< 1 ppm). Total REEs are, however, very high relative to all other AMD products.

The geochemical speciation and saturation modelling of AMD samples indicates that goethite is always supersaturated in all waters regardless of their pH. The degree of supersaturation increases with increasing pH. This supersaturation explains why goethite is the dominant precipitate throughout the mine despite large fluctuations in groundwater chemistry caused by flushing during periods of heavy rainfall. In order to predict the behaviour of the amorphous Fe oxyhydroxide, a saturation index was calculated for $Fe(OH)_3$ (this represents the closest analogue available in the EQ3NR database). EQ3NR predicts $Fe(OH)_3$ is undersaturated at low pH values and saturated or supersaturated in the near-neutral pH (pH 6 to 8) drip-waters that form the amorphous iron oxyhydroxide stalactites. Although goethite is also predicted to be supersaturated (S.I.=7.4 max.) in these drips, it is not detected in the associated stalactites and X-ray amorphous Fe oxyhydroxide material has preferentially precipitated. This suggests that the precipitation of amorphous Fe oxyhydroxide, not goethite, is kinetically favoured at near-neutral pH. In contrast, in the AMD, goethite rather than amorphous Fe oxyhydroxide is precipitated. Melanterite and gypsum are always undersaturated in the groundwaters, although the SI for melanterite increases by a factor of two with a decrease in pH, bringing melanterite slightly closer to saturation. Gypsum approaches saturation in the AMD. This explains why, under slight evaporation on the walls of the mine, melanterite and gypsum become saturated and readily develop the extensive crusts observed.

Pearce & Kemp - A Geochemical Study of Acid Mine Drainage from a Pyrite Mine, North Wales.

DISCUSSION

The formation and distribution of goethite and amorphous Fe oxyhydroxide in the mine appear to be controlled by the kinetics of precipitation. In the inflowing drips, where amorphous Fe oxyhydroxide is saturated, it precipitates instead of goethite, despite the greater degree of goethite supersaturation.

The formation of goethite in Fe-rich waters, particularly of low pH has been well documented [e.g. 9, 10 and 11]. It is widely considered that goethite is an ageing product of ferrihydrite or jarosite ($KFe_3[SO_4]_2[OH]_6$) [e.g. 9]. Other studies [12, 13] have shown that ferrihydrite is the dominant phase to precipitate from AMD. However we have found no evidence at the Cae Coch site that goethite has formed following transition from an earlier phase. The stratified nature of the goethite precipitate and the close proximity to the acidic stream suggest that the goethite has precipitated directly from solution. This is further supported by the geochemical modelling which indicates that goethite is supersaturated in these groundwaters and amorphous iron oxyhydroxide is undersaturated.

Goethite precipitation from solution following ferrihydrite dissolution has been achieved in the laboratory [10]. It was found that goethite precipitation is most favoured when the concentration of Fe^{III} is at a maximum. In addition this study (op cit.) found that goethite formation is also favoured when Fe^{III} occurs in monovalent complexes, since it is easier to produce free Fe^{III} ions when in a monovalent instead of polyvalent complex. EQ3NR modelling predicts the uncomplexed Fe^{3+}_{aq} ion and $Fe_3(OH)_4{}^{5+}_{aq}$ complex should be present in similar proportions in the AMD. This will favour goethite formation. Hence, goethite formation is possible by direct precipitation from acid groundwaters, particularly if amorphous Fe oxyhydroxide is undersaturated, as suggested by the geochemical modelling.

Atypically for such environments [15, 16], jarosite is not precipitated in large quantities at Cae Coch. Although K is not present in the groundwaters, there is sufficient Na present for natrojarosite SI calculations to be made. These calculations indicate that in the AMD natrojarosite is, in fact, supersaturated. It is possible that goethite precipitation is kinetically favoured and that significant Fe^{III} is removed before natrojarosite can precipitate or that any jarosite formed is redissolved by more dilute groundwaters during periods of higher flow. Jarosite was present associated with gypsum encrustations on drier, weathered shale surfaces.

Graphical representations of the trace element concentrations in Fe-rich precipitates relative to their associated groundwaters are presented in double logarithmic diagrams (after [12]). Several distinct groups of elements can be identified in the goethite sample (Figure 1). Fe, Al and Ca dominate in goethite compared to the adjacent AMD stream. Li and Sr concentrations are one order of magnitude greater in goethite. Ba, Zr and Cr concentrations are enriched by three orders of magnitude in the goethite relative to the groundwater. V and Cu are enriched by four orders of magnitude in the goethite sample. Hence there is significant enrichment in the goethite of many trace elements relative to the groundwater. The REE concentrations are enriched by an order of magnitude in the goethite sample relative to the water. For the amorphous Fe oxyhydroxide sample (Figure 2) the dataset is greatly reduced, since many elements are below detection in the water sample. This precipitate shows similar partition of trace elements between solid phase and groundwater to the goethite sample with Fe and Ca concentrations dominating in the solid. Mn, Ba and Zn concentrations are enriched by four to five orders of magnitude in the amorphous Fe oxyhydroxide. U concentration is approximately three orders of magnitude greater in the amorphous Fe oxyhydroxide.

As many of the trace elements present in the amorphous Fe oxyhydroxide precipitates are at concentrations below detection in the associated mine waters, the relative sorption is much greater than for the goethite sample (although the absolute concentrations for some elements are higher in the goethite). The relatively higher partition of trace elements from the near-neutral drips by the amorphous Fe oxyhydroxide compared to trace element partition by goethite from the AMD is the result of coprecipitation and sorption. pH has significant influence on both of these processes. Coprecipitation of trace metals such as Cd, Cu, Pb and Zn with amorphous Fe oxyhydroxide is known to be significant [17]. In addition, sorption processes are likely to be very significant and are likely to continue once coprecipitation has finished [18]. Sorption processes are determined by the presence of an "adsorption edge" below which little sorption occurs [12 and references therein]. Sorption will be much reduced in the goethite since the pH is below its adsorption edge. The greater surface area of the amorphous Fe oxyhydroxide will also mean that sorption will be greater. However, it must be remembered that direct comparisons of the uptake of trace elements by amorphous Fe oxyhydroxide relative to goethite can not be made since the waters from which coprecipitation and sorption are occurring are very different. Only the magnitude of the uptake of the solid relative to its associated groundwater can be compared.

Pb is not significantly sorbed by either goethite or amorphous Fe oxyhydroxide. Pb and Co are below detection limit in the waters but Co sorbs on to both goethite and amorphous Fe oxyhydroxide. This contradicts previous studies which indicate that Pb should coprecipitate with Fe at the same pH [19].

Total REE are enriched by two orders of magnitude in goethite relative to the AMD from which it precipitates. The amorphous Fe oxyhydroxide contains significant enrichment of REE relative to the roof drips in which no REE were detected. The most significant sink for these elements is gypsum which contains at least five times higher total REE than amorphous Fe oxyhydroxide or goethite. There is little data available on the typical abundances of REE in gypsum. However some evidence from fracture filling gypsum indicates that it can be an effective sink for REE [20]. This is very significant to understanding the REE geochemistry of acidic minewaters.

The chondrite-normalised REE pattern [21] for the amorphous Fe oxyhydroxide sample indicates preferential HREE enrichment. This is in contrast to gypsum in which the LREE are preferentially enriched (Figure 3). REE are therefore fractionated under AMD conditions, with HREE being preferentially removed from solution by amorphous Fe oxyhydroxide and the LREE remaining in solution until they are incorporated into gypsum efflorescences. LREE enrichment has also been reported in fracture filling gypsum precipitating from saline fluids [20]. Both REE chondrite-normalised patterns are significantly different from the AMD patterns, which further emphasises the preferential and specific removal of REE from solution by the gypsum and amorphous Fe oxyhydroxide. This is in accord with data obtained at the Poços de Caldas natural analogue site [22]. Here the highest total REE were found in acidic, sulphate-rich, oxidising, surface waters. Sorption onto amorphous Fe oxyhydroxide was also determined to be significant in these waters. It was also suggested by Miekely et al. (1992) that the stability of REE(III)-sulphate complexes would mean that sorption was suppressed. At Cae Coch this may account for the higher concentrations of REE found in the gypsum relative to the amorphous Fe oxyhydroxide. Although EQ3/NR modelling predicts the dominant aqueous species in the AMD to be REE(III) and not a sulphate complex, this is probably due to a lack of data in the database. The similarity of REE(III)-sulphate stability constants means that significant fractionation of the REE should not take place. However, during gypsum precipitation fractionation is clearly occurring. The lack of a Ce anomaly in the REE patterns is unusual since it would be expected under the low pH and high Eh conditions of the AMD to exist as Ce^{4+} which is very immobile. The lack of a Ce anomaly suggests that Ce does in fact remain mobile under AMD conditions.

Th is not removed from solution by a specific precipitate, remaining at higher concentrations in the AMD relative to the precipitates. Similarly, and surprisingly, U is not removed from solution except by possible nonspecific adsorption in the amorphous Fe oxyhydroxide A strong affinity between U and Fe oxyhydroxides has been well established and it is unusual to find U apparently remaining in solution under these conditions. Since U is predicted to occur predominantly as

$UO_2SO_4(aq)$, UO_2^{2+} and $UO_2(SO_4)_2^{2-}$ complexes the formation of these complexes may reduce sorption.

SUMMARY

The multidisciplinary approach used in the study of the precipitates from the Cae Coch pyrite mine has identified the formation of goethite directly from Fe-rich, low pH groundwaters. The relative importance of goethite, amorphous Fe oxyhydroxide and gypsum in removing trace elements from solution has been determined. The relative sorption of trace elements from solution by goethite in the natural system at Cae Coch is in general agreement with that determined in laboratory studies performed by other workers. Both the goethite and amorphous Fe oxyhydroxide are important sinks for Co, Ni, Ba and REE with the amorphous Fe oxyhydroxide having particularly high sorption capabilities. In addition, it was found that fractionation of the REE occurs, with the LREE being incorporated into gypsum. These phases therefore play an important rôle in the removal of elements such as Co, Ni, REE and Ba, from acid mine waters.

This study has demonstrated that the combination of several analytical techniques and a systematic approach to sampling can be very useful in establishing the nature of fluid-rock interactions that lead to acid mine drainage. In addition, it is possible to establish which precipitates often associated with acid mine drainage are likely to act as sinks for heavy metals and other trace elements and influence or control its environmental impact.

ACKNOWLEDGEMENTS

This work was funded by UK Nirex Ltd under the Nirex Safety Assessment Research Programme (NSARP). The authors would like to thank Dr. C. Rochelle for performing the EQ3NR calculations and providing valuable advice on their interpretation and Dr T.K. Ball with help in the field. The authors are also indebted to Mr. A. E. Milodowski for his constructive criticism and encouragement. This paper is published with the approval of the Director of the British Geological Survey, NERC.

REFERENCES

1. Ferris, F.G., Tazaki, K. and Fyfe, W.S. Fe oxides in acid mine drainage environments and their association with bacteria. Chemical Geology. Vol.74. pp.321-330. (1989).

2. Bigham, J.M., Schwertmann, U., Carlson, L. and Murad, E. A poorly crystallised oxyhydroxysulfate of Fe formed by bacterial oxidation of Fe(II) in acid mine waters. Geochimica et. Cosmochimica Acta. Vol.54. pp.2743-2758. (1990).
3. Lim-Numez, R. and Gilkes, R.J. Acid dissolution of synthetic metal containing goethites and hematites. In: L. G. Schultz, H. van Olphen and F. A. Mumpton (Editors), Proceedings of the International Clay Conference. pp.197-204, Denver. (1987).
4. Moses, C.O., Nordstrom, D.K., Herman, J.S. and Mills, A.L. Aqueous pyrite oxidation by dissolved oxygen and ferric Fe. Geochimica et Cosmochimica Acta. Vol.51. pp.1561-1571. (1987).
5. Ball, T.K. and Bland, D.J. The Cae Coch volcanogenic massive sulphide deposit, Trefriw, North Wales. Journal Geology Society London. Vol.142. pp.889-898. (1985).
6. Wolery, T.J. EQ3NR, a computer program for geochemical aqueous speciation-solubility calculations: Theoretical manual, users' guide and related documentation (version 7). Lawrence-Livermore National Lab. Report. UCRL-MA-110662. Part III. (1992).
7. Schwertmann, U. and Taylor, R.M. Iron oxides. In: J. B. Dixon and S. B. Weed (Editors), Minerals in Soil Environments. pp.145-180, Soil Science Society of America, Madison. (1977).
8. Schwertmann, U. Is there amorphous iron oxides in soils? Abstract from Annual Meeting of Soil Society of America, Fort Collins, Colorado. (1979).
9. Nordstrom, D.K. Aqueous pyrite oxidation and the consequent formation of secondary iron minerals. In: J. A. Kittrick, D. S. Fanning and L. R. Hossner (Editors), Acid Sulfate Weathering. pp.37-56. Soil Science Society of America. (1982).
10. Schwertmann, U. and Murad, E. Effect of pH on the formation of goethite and hematite from ferrihydrite. Clays and Clay Minerals. Vol.31(4). pp.277-284. (1983).
11. Carlson, L. and Schwertmann, U. Natural ferrihydrites in surface deposits from Finland and their association with silica. Geochimica et Cosmochimica Acta. Vol.45. pp.421-429. (1981).
12. Chapman, B.M., Jones, D.R. and Jung, R.F. Processes controlling metal ion attenuation in acid mine drainage. Geochimica et. Cosmochimica Acta. Vol.47. pp.1957-1973. (1983).
13. Fillipek, L.H., Nordstrom, D.K. and Ficklin, W.H. Interaction of acid mine drainage with waters and sediments of West Squaw Creek in the West Shasta Mining District, California. Environmental Science and Technology. Vol.21(4). pp.388-386. (1987).
14. Brady, K.S., Bigham, J.M., Jaynes, W.F. and Logan, T.J. Influence of sulfate on Fe-oxide formation: Comparisons with a stream receiving acid mine drainage. Clays and Clay Minerals. Vol.34(3). 266-274. (1986).
15. Bladh, K.W. The formation of goethite, jarosite, and alunite during the weathering of sulphide-bearing felsic rocks. Economic Geology. Vol.77. pp.176-184. (1982).

16. Blowes, D.W., Reardon, E.J., Jambor, J.L., Cherry, J.A. The formation and potential importance of cemented layers in inactive sulphide mine tailings. Geochimica et Cosmochimica Acta. Vol.55. pp.965-978. (1991).
17. Benjamin, M.M., Hayes, K.F. and Leckie, J.O. Removal of toxic metals from power-generation waste streams by adsorption and coprecipitation. Journal WPCF. Vol.54(11). pp.1472-1481. (1982).
18. Robinson, G.D. Adsorption of copper, zinc and lead near sulphide deposits by hydrous manganese-Fe oxide coatings on stream alluvium. Chemical Geology. Vol.33. pp.65-79. (1981).
19. Karlsson, S., Sanden, P. and Allard, B. Environmental impacts of an old mine tailings deposit-metal adsorption by particulate matter. Nordic Hydrology. Vol.18 pp.313-324. (1987).
20. Mungall, J.E., Frape, S.K. and Gigson, I.L. Rare-earth abundances in host granitic rocks and fracture-filling gypsum associated with saline groundwaters from a deep borehole, Aitokan, Ontario. Canadian Mineralogist. Vol.25. pp.539-543. (1987).
21. Wedepohl, K.H. The handbook of geochemistry. Springer-Verlag, Berlin. (1978).
22. Miekeley, N., Coutinho de Jesus, H., Porto da Silveira, C.L., Linsalata, P. and Morse, R. Rare-earth elements in groundwaters from the Osamu Utsumi mine and Morro do Ferro analogue study sites. In: N. A. Chapman, I. G. McKinley, M. E. Shea and J. A. T. Smellie (Editors), The Poços de Caldas Project: Natural Analogues of Processes in a Radioactive Waste Repository. Journal of Geochemical Exploration. Vol.45. pp.365-387. (1992).

Pearce & Kemp - A Geochemical Study of Acid Mine Drainage from a Pyrite Mine, North Wales.

Table 1. Geochemical data for selected water samples. All concentrations in ppm, except REE, U and Th in ppb.

Sample	Inflow[1] CC6[3]	Inflow CC8[4]	Inflow CC11[4]	Inflow CC12[4]	AMD[2] CC13[4]	AMD CC5[3]	AMD CC2[3]	AMD CC3[3]	AMD CC14[4]	AMD CC7[3]
Field pH	6.0	7.7	7.8	7.8	2.7	2.6	n/a	2.1	2.5	
Eh (mV)	302	208	868	586	745	872	n/a	547	699	807
Ca	43.5	41.6	49.9	51.7	76.2	139.7	159.8	41.4	205.5	110.8
Mg	3.0	5.4	3.6	3.5	21.0	27.0	29.7	4.2	42.3	32.1
Na	8.9	16.6	9.5	13.8	8.1	10.4	9.6	10.2	9.6	8.9
K	0.6	0.7	0.5	0.6	0.0	0.0	0.0	0.6	0.0	0.0
HCO3	0	176	173	157	0	0	0	0	0	0
Cl	10.6	8.8	9.8	11.6	17.9	0.0	0.0	11.1	16.4	0.0
SO4	21.6	13.9	12.8	16.3	1010.0	1620.0	2460.0	31.8	5110.0	3110.0
NO3	0.3	0.1	0.0	0.0	0.0	0.0	0.0	1.0	0.0	0.0
F	0.2	0.2	0.2	0.2	0.6	0.6	0.0	0.2	0.0	0.0
TOC	3.1	2.0	2.0	0.9	0.0	2.8	2.7	4.9	2.7	3.3
TIC	26.8	29.7	27.9	23.8	0.0	0.0	0.0	24.2	0.0	0.0
P	0.0	0.0	n/a	0.0	0.2	0.5	0.5	0.0	1.0	1.2
Total S	5.9	4.7	4.6	6.3	295.0	630.0	731.7	8.9	1390.0	958.9
Si	6.8	5.1	6.1	5.2	20.2	25.1	31.5	5.6	24.2	17.5
Ba	0.11	0.12	0.12	0.10	0.03	0.02	0.02	0.08	0.01	0.01
Sr	0.14	0.27	0.16	0.21	0.10	0.20	0.18	0.19	0.19	0.15
Mn	0.19	0.02	0.19	0.06	1.92	1.25	1.55	0.04	3.05	1.80
Total Fe	0.90	0.10	0.27	0.10	171.80	476.20	527.30	0.00	1460.00	849.90
Fe2+	1.90	0.10	0.98	0.07	62.99	50.90	0.30	12.00	117.00	13.40
Al	0.00	0.00	0.00	0.00	26.65	46.59	51.90	0.07	84.21	51.96
Co	0.00	0.00	0.00	0.00	0.00	0.00	0.00	0.00	0.00	0.00
Ni	0.00	0.00	0.00	0.00	0.00	0.10	0.15	0.00	0.37	0.36
Cu	0.00	0.00	0.00	0.00	0.00	0.02	0.03	0.00	0.16	0.20
Zn	0.01	0.00	0.00	0.00	0.19	0.39	0.44	0.00	0.94	0.72
Cr	0.00	0.00	0.00	0.00	0.28	0.68	0.74	0.00	1.88	1.17
Zr	0.00	0.00	0.00	0.00	0.01	0.03	0.03	0.00	0.08	0.05
Cd	0.00	0.00	0.00	0.00	0.00	0.01	0.01	0.00	0.03	0.03
Pb	0.00	0.00	0.00	0.00	0.00	0.00	0.00	0.00	0.00	0.00
V	0.00	0.00	0.00	0.00	0.10	0.19	0.22	0.00	0.56	0.34
Li	0.00	0.00	0.01	0.00	0.07	0.10	0.10	0.00	0.17	0.09
As	0.00	1.80	0.20	0.00	2.30	0.00	0.00	0.00	213.70	0.00
Y	0.00	0.06	0.04	0.08	23.20	40.72	0.00	35.68	76.60	68.09
La	0.00	0.00	0.00	0.03	20.70	31.50	0.00	30.51	48.90	43.35
Ce	0.00	0.02	0.03	0.05	45.40	76.15	0.00	76.84	112.70	110.43
Pr	0.00	0.00	0.00	0.00	6.10	10.33	0.00	10.21	15.70	14.63
Nd	0.00	0.00	0.00	0.00	29.80	47.62	0.00	46.58	76.60	66.29
Sm	0.00	0.08	0.08	0.06	7.10	11.24	0.00	11.16	18.90	16.90
Eu	0.00	0.06	0.05	0.04	2.01	1.81	0.00	3.47	5.95	4.88
Gd	0.00	0.00	0.00	0.00	7.06	10.63	0.00	10.97	20.20	17.22
Tb	0.00	0.00	0.00	0.00	1.10	2.02	0.00	1.70	3.19	2.86
Dy	0.00	0.00	0.00	0.00	6.05	5.69	0.00	10.04	18.90	16.59
Ho	0.00	0.00	0.00	0.00	1.21	0.81	0.00	1.89	3.61	3.07
Er	0.00	0.00	0.00	0.00	3.17	4.99	0.00	5.34	10.20	8.32
Tm	0.00	0.00	0.00	0.00	0.45	0.66	0.00	0.76	1.70	1.11
Yb	0.00	0.00	0.00	0.00	2.67	1.16	0.00	4.75	8.57	6.57
Lu	0.00	0.00	0.00	0.00	0.35	5.95	0.00	0.63	1.06	0.85
Th	0.00	0.00	0.00	0.00	0.00	0.00	0.00	1.43	4.46	6.99
U	5.74	13.60	6.00	2.20	1.36	5.74	5.99	6.03	7.23	10.01
ΣREE	0.00	0.16	0.16	0.18	133.17	218.47	0.00	214.85	346.18	313.07

1 Inflow waters are those of near-neutral pH typically occurring as roof drips and at higher parts of the mine.
2 AMD = Acid mine drainage waters, pH <3.0, formed due to interaction with oxidising pyrite within the mine.
3 Samples collected January 1991. 4 Samples collected June 1991. n/a Not analysed

Table 2. Major element (wt%), trace element (ppm) and REE (ppm) concentrations for precipitates of AMD.

	Pyrite SJK71	Goethite SJK56	Goethite SJK80	Gypsum SJK49b	Gypsum SJK59	Melanterite SJK54b	Am. Fe oxy.[1] SJK57a
Al_2O_3	0.22	0.11	1.00	0.11	0.11	0.00	0.05
Fe_2O_3	77.09	86.62	70.73	0.87	9.91	34.70	67.25
MgO	0.00	0.03	0.16	0.03	0.04	0.19	0.05
CaO	0.12	0.2	0.23	30.68	27.41	0.27	2.81
Na_2O	0.08	0.00	0.00	0.08	0.86	0.00	0.01
K_2O	0.01	0.00	0.00	0.02	0.05	0.00	0.01
TiO_2	0.00	0.17	0.11	0.01	0.00	0.01	0.00
P_2O_5	0.08	0.26	0.17	0.13	0.13	0.04	0.25
MnO	0.00	0.00	0.01	0.00	0.00	0.01	1.72
Total	77.60	87.39	72.41	31.93	38.51	35.22	72.15
Ba	28	8	29	25	27	25	2428
Co	26	29	28	11	13	25	29
Cr	25	35	37	10	13	13	31
Cu	19	29	63	8	25	115	8
Li	2	2	8	6	8	1	4
Nb	1	0	0	1	1	0	0
Ni	5	0	16	2	3	30	226
Sc	0	0	2	2	1	0	0
Sr	4	1	2	148	155	1	190
V	49	172	84	6	12	23	48
Y	1	2	5	9	6	1	138
Zn	24	37	73	7	16	32	87
Zr	14	14	12	5	3	6	13
Pb	486	<10	<10	<10	<10	16	235
Cd	<1	<1	1	1	<1	<1	<1
La	0.26	0.24	2.31	50.75	57.43	0.23	5.45
Ce	0.31	1.28	6.62	136.16	114.56	0.26	6.85
Pr	0.01	0.42	1.08	17.07	13.29	0.06	0.96
Nd	0.2	1.1	5.2	68.6	52.7	0.3	4.7
Sm	0.08	0.03	1.04	9.74	7.04	0.13	0.92
Eu	0.01	0.04	0.25	1.58	1.1	0.01	0.37
Gd	0.01	0.36	1.24	4.31	3.49	0.03	2.7
Dy	0.03	0.11	0.89	2.00	1.50	0.00	5.6
Ho	0.01	0.02	0.15	0.29	0.22	0.01	1.65
Er	0.07	0.14	0.48	0.80	0.56	0.07	6.46
Yb	0.05	0.06	0.32	0.26	0.15	0.00	6.73
Lu	0.00	0.03	0.05	0.05	0.02	0.01	1.44
Y	0.3	0.5	4.1	6.4	5.0	0.1	133.4
U	<0.65	<0.5	<0.7	<0.7	<0.5	<0.4	3.0
Th	<0.92	<0.8	<0.69	<0.8	<0.6	<0.4	<1.0

1 Am. Fe. Oxy = Amorphous iron oxyhydroxide.

Pearce & Kemp - A Geochemical Study of Acid Mine Drainage from a Pyrite Mine, North Wales

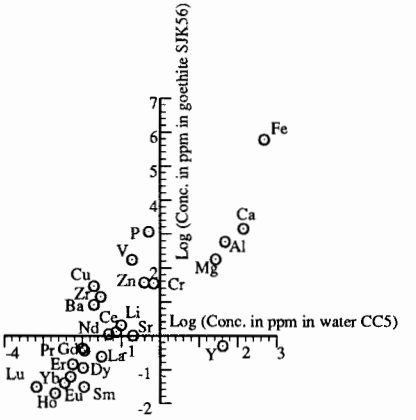

Figure 1: Double logarithmic plot of elemental concentrations in goethite relative to acid mine drainage sample CC5.

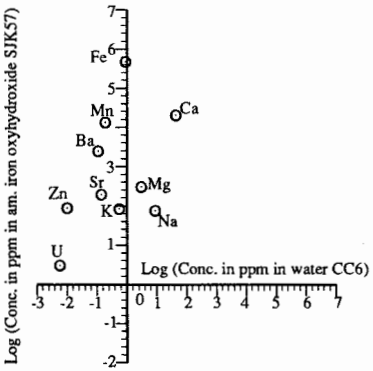

Figure 2: Double logarithmic plot of elemental concentrations for amorphous iron oxyhydroxide stalactite relative to roof drip CC6.

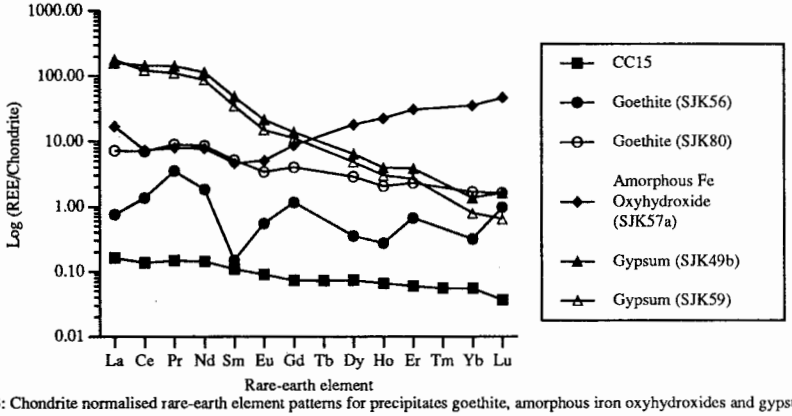

Figure 3: Chondrite normalised rare-earth element patterns for precipitates goethite, amorphous iron oxyhydroxides and gypsum